Proceedings of the 12th International Symposium UFPS, Vilnius, Lithuania 2004

Formation of Iron-Containing Clusters in Silica of Predetermined Porosity

I. Šimkiene[a,*], M. Baran[b], G.-J. Babonas[a,c], R.-A. Bendorius[a,c], A. Rėza[a], R. Szymczak[b], P. Aleshkevych[b], R. Šustavičiūtė[a] and R. Tamaševičius[a]

[a]Semiconductor Physics Institute, Goštauto 11, 01108 Vilnius, Lithuania

[b]Institute of Physics, PAS, al. Lotników 32/46, 02-668 Warszawa, Poland

[c]Vilnius Gediminas Technical University, Saulėtekio 11, 10223 Vilnius, Lithuania

Iron-containing nanoparticles and clusters were formed in silica with porosity, which was predetermined by different procedures of sol-gel technology and the chemical composition of precursors. Bulk and layer-type samples of different porosity were synthesized and investigated. The morphology, magnetic, and optical properties were studied to characterize the samples and to analyze the formation of Fe-oxides. Experimental results showed that both Fe_2O_3 and Fe_3O_4 were formed in the samples and that their relative amount was dependent on preparation technology.

PACS numbers: 61.46.+w, 75.75.+a, 78.66.–w

1. Introduction

Recently, the systems of iron-containing clusters embedded in oxide silica matrix have been widely studied due to their potential applications [1], in particular as magnetic recording media. However, the magnetic behavior of iron-containing nanoparticles was strongly dependent on technology of sample preparation [2]. Magnetite (Fe_3O_4) nanorods and porous hematite (α-Fe_2O_3) nanorods were prepared [3] through hydrolysis of $FeCl_3$ and $FeSO_4$ solutions. Nanoparticles of α-Fe_2O_3 with a closed cage structure were formed [4] by a low-temperature hydrothermal method from aqueous solution of $FeCl_3$ and cetyltrimethylammonium bromide (CTAB).

The sol-gel method is mostly perspective for preparation of magnetic nanocomposites embedded in dielectric matrix-like silica. However, a gelation process and the formation of final nanocomposites were strongly influenced [5] by the surface-to-volume ratio and later heat treatments. Therefore, it is reasonable

*corresponding author; e-mail: irena@pfi.lt

to assume that the porosity of matrix plays a crucial role in the formation of iron-containing particles and clusters.

In this work Fe-containing clusters were formed and investigated in silica of porosity, which has been predetermined by different procedures of sol-gel technology and by varying the composition of precursors. Three groups of samples were synthesized and investigated: (i) bulk sol samples of high porosity prepared by a hydrolysis of tetraethoxysilane (TEOS)-based solutions; (ii) low-porosity Fe-containing silica layers produced by sol-gel spin-on technique on Si substrates using precursors TEOS+$FeCl_3$; (iii) high-porosity Fe-containing silica layers prepared by spin coating on Si substrates from precursors with surfactant CTAB.

Morphology of synthesized samples was studied by scanning electron microscopy (SEM) and atomic force microscopy (AFM). The magnetic and optical properties were investigated to characterize the samples and to analyze the formation of Fe-oxides.

2. Experimental

Bulk samples of iron-containing silica were prepared by mixing the aqueous solution of $FeCl_3$ and TEOS (20 ml $Si(C_2H_5O)_4$ + 40 ml C_2H_5OH + 4 ml H_2O + 0.1 ml HCl) in volume ratio 1:3. Several drops of ammonia were added to reach a pH-value equal to 5. Clear sols were obtained in ultrasound bath in 1 h and gelated at 300 K in air for 10 days. The gels were dried at 100°C for 8 h and annealed in Ar or hydrogen at 550°C for 2 h.

The sol of composition described above was used as precursor for spin-coating of Si substrates (n-Si (100)-oriented wafers, 0.5 Ω cm). Si substrates were previously coated by two silica layers from TEOS solution making use of the spin-on technique. Each silica layer of thickness ≈ 150 nm were dried at 300°C for 1 h. The structure of the samples represent a multi-layer stack on substrate, two pure silica layers and two Fe-doped silica layers. The samples were annealed in air, Ar or H_2 at 500°C for 2 h.

The other samples were obtained by sol-gel spin-on technique from precursors with surfactant CTAB. In one case 0.84 g $FeCl_3$, 0.6 g CTAB were dissolved in 40 ml H_2O and stirred in the ultrasound bath for 30 min until homogeneous yellow sol was formed. The solution was deposited on substrate in centrifuge (2500 rpm). In the second case the solution described above was mixed with TEOS in volume ratio 1:1 and used for spin-coating. The samples were dried at 80°C for 4 h and some samples were annealed in air at 550°C for 1 h.

Magnetic properties of complex structures were studied using a commercial SQUID magnetometer (MPMS-5, Quantum Design). The magnetization was measured in the temperature range 5–300 K in magnetic fields up to 50 kOe. The magnetic field was oriented in the plane of the films.

The optical properties of synthesized samples were studied by null- and spectroscopic ellipsometry, photoluminescence, and optical transmission measurements. Spectroscopic ellipsometry measurements were carried out at 300 K in

the range 1–5 eV by means of a photometric ellipsometer with rotating analyzer. The experimental data were analyzed in a model of multilayer structure. The ellipsometric parameters Ψ and Δ were directly calculated by solving the Maxwell equations using the transfer matrix technique.

Photoluminescence was excited by Ar-ion laser ILT5000 (50 mW at 488 nm). The photoluminescence spectra were obtained by means of monochromator MDR-12 using the grating of 1200 lines/mm.

The physical properties of iron-containing silica layers were correlated with the structural features studied by SEM and AFM techniques.

3. Results and discussion

3.1. Bulk samples

Different iron oxides can be formed in bulk samples. When precursor with $FeCl_3$ was used, β-FeOOH was usually formed which transformed to α-Fe_2O_3 after heat treatment [6]. However, in contrast to other studies, in this work, the colloidal TEOS solution was used in which polymer-like chains O–Si–O–Si have been already formed. For this reason, the final composites could differ from those observed earlier [6] and various iron oxides could be formed.

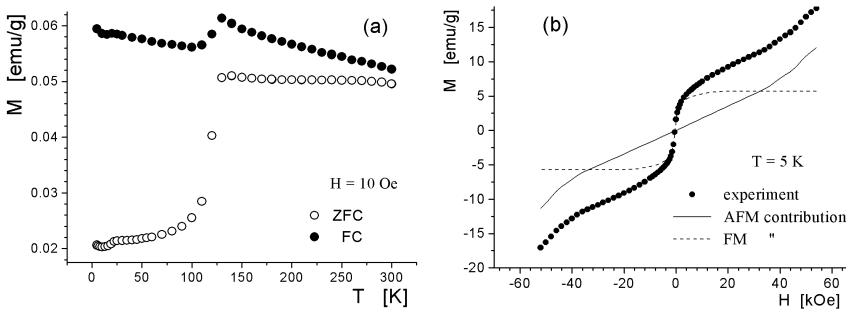

Fig. 1. Temperature (a) and magnetic field dependence (b) of magnetization for bulk samples annealed in Ar.

Figure 1 illustrates the magnetic properties of the bulk samples annealed in Ar. The temperature dependence of magnetization at low magnetic field of 10 Oe and the difference between field-cooled (FC) and zero-field cooled (ZFC) data were similar to those observed in [7] for large nanoparticles of magnetite of size 150 nm. A phase transition occurs near 130 K, which correlates to the Verwey transition in Fe_3O_4. At higher magnetic fields (20 and 50 kOe) the magnetization increased but the difference between FC and ZFC as well as the feature at 130 K disappeared. Some peculiarity in $M(T)$ behavior was also observed at $\approx$ 20 K. It should be noted that the characteristic Verwey temperature was found [7] to shift from 98 to $\approx$ 20 K as the size of nanoparticles was reduced from 150 to 50 nm. However,

the peculiarities at ≈ 130 K and ≈ 20 K are of different origin because of their quite different behavior at magnetic field changes.

Magnetic field dependence of magnetization $M(H)$ (Fig. 1) has shown a lack of saturation (both at 5 and 300 K) and a bend (at 5 K) in about 40 kOe, which could be interpreted as the field-induced magnetic phase transition. $M(H)$ approached at 300 K the value of 6 emu/g, which is significantly lower than that for nanoparticles of pure Fe_3O_4 [7]. All the facts could suggest that beside the ferrimagnetic contribution there is also some of antiferromagnetic (AFM) type, let us say of α-Fe_2O_3 or FeSi. In this case the kink at 20 K for $M(T)$ in high magnetic fields could be ascribed to the Morin-type transition from weak FM to AFM structure in α-Fe_2O_3 with a large shift of the characteristic temperature due to the formation of nanoparticles. The hysteresis loop measurements have shown that the coercive force amounts to ≈ 500 and 200 Oe at 5 and 300 K, respectively. The remanence-to-saturation ratio is smaller than 0.5 indicating the existence of interparticle interactions of AFM nature.

The magnetization of H_2-annealed bulk samples was considerably higher than that of Ar-annealed samples. No clear manifestation of phase transition was observed though some peculiarity was noticed at ≈ 50 K. The FM/ferrimagnetic or supermagnetic contributions were expected from the temperature dependence $M(T)$, which was quite similar to that [8] for oxide-coated Fe cluster assemblies of 5–10 nm in size. The FC magnetization weakly depended on temperature and the remanence decreased only by 20% as the temperature increased from 5 to 300 K indicating a high value of the Curie temperature. The magnetic field dependence of magnetization was similar at 5 and 300 K showing at ≈ 10 kOe the tendency for saturation at 45 emu/g. The latter value was smaller than that (76 emu/g) for bulk γ-Fe_2O_3 but was higher than that for nanoparticles of ≈ 10 nm [1]. The coercive force was equal to ≈ 100 Oe and was weakly dependent on temperature as was determined for silica-coated Fe particles of 35 nm [9]. It should be noted that in the latter case the saturation magnetization at 5 K was strongly dependent on calcination temperature for a constant particle size [9].

As follows from the data presented above, the most probable explanation of the observed experimental data is that the bulk samples contain both magnetite (Fe_3O_4) and hematite (α-Fe_2O_3) particles. The maghemite (γ-Fe_2O_3) particles were usually accompanied by hematite in Fe-oxide — silica aerogel and xerogel samples [10]. In the investigated bulk samples most probable contributions were originated from magnetite and hematite in Ar-annealed samples whereas maghemite and Fe nanoparticles coated by iron oxides contribute mainly to magnetization of H_2-annealed samples.

3.2. Dense Fe-containing silica layers on Si substrates

In the silica layers deposited on Si substrates by sol-gel spin-on technique large clusters and small nanosized particles were observed. A granular structure

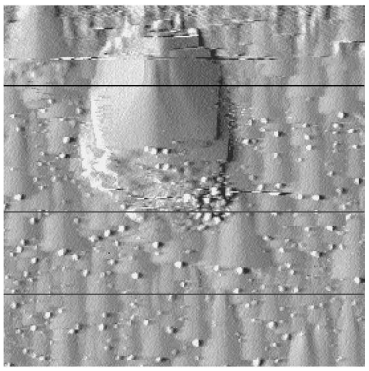

Fig. 2. AFM image of Fe-containing silica layer annealed in H_2. The area shown is 5×5 μm^2.

with grains of 1–2 μm in size and $\approx$ 200 nm in height was observed on the surface of layers annealed in air or Ar. Large defects of size 20−40 μm with a higher Fe-content [11] were also formed. In the silica layers annealed in H_2 (Fig. 2) the grains were smaller (200–500 nm in size) though some larger grains (up to 1 μm) were also noticed. Nanosized particles (Ø 10−40 nm) could be assigned to iron/iron oxide formations.

Silica layers deposited on Si substrates by sol-gel spin-on technique were denser than bulk silica samples. The refractive index of silica layers prepared from acid-based precursors with pH $\approx$ 2 was equal to 1.42−1.43 as followed from null--ellipsometry measurements at 633 nm. Taking into account the refractive index of thermal oxide ($n = 1.45$) the porosity of silica layers were estimated to be of order 5–10%.

The photoluminescence spectra (Fig. 3) were different for samples produced under various technological conditions. In the case of precursors TEOS+$FeCl_3$ without surfactant, the photoluminescence bands at $\approx$ 675, 750, and 825 nm were observed for annealed samples. These bands were resolved in the spectra of almost

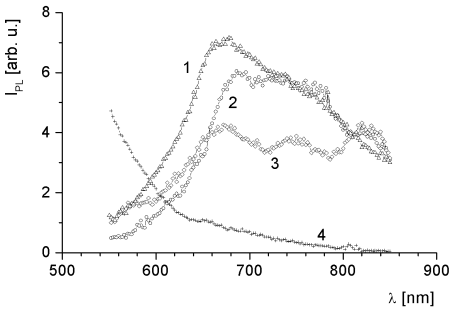

Fig. 3. Photoluminescence spectra of Fe-containing silica layers produced from precursors with (1) and without (2–4) surfactant, with pH-value $\approx$ 2 (2) and $\approx$ 5 (3, 4) at $FeCl_3$:TEOS ratio 1:3 (3, 4) and 1:1 (2) annealed in air (2, 3) and H_2 (4).

all the samples but with various relative intensities. At an increase in Fe-amount, broad band at 670–800 nm was formed. In the samples prepared from TEOS-based precursors with surfactant the band at 670 nm was dominant.

The difference in the fine structure of photoluminescence spectra is most probably caused by the formation of various Fe oxides in the silica layers. The spectral position of the photoluminescence band at ≈ 670 nm correlates with the absorption edge of Fe_2O_3 [12]. The photoluminescence bands at longer wavelengths can be related to the optical features in Fe_3O_4 [13] and are most developed in the samples with the largest iron amount in precursor. In the photoluminescence spectra of the samples annealed in H_2 the contribution of band at $\lambda < 550$ nm was determined and could be related to the formation of Fe-containing nanoparticles in silica layers.

Spectroscopic ellipsometry data were well described by a multi-layer model, which took into account the presence of different iron oxides in silica and in-depth variation of porosity. Figure 4 illustrates ellipsometric data for Fe-doped silica layer prepared from base-based precursor and annealed in H_2. The sample was modeled by the stack of porous layers of Fe particles, non-homogeneous composite layers of Fe_3O_4 and SiO_2, and substrate.

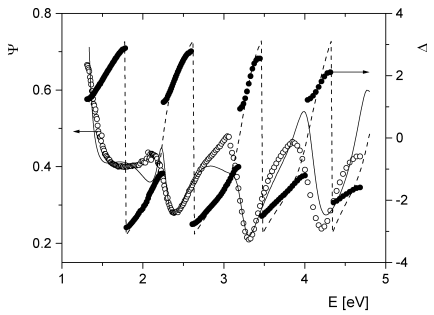

Fig. 4. Experimental (points) and modeled (curves) spectra of ellipsometric parameters for Fe-containing silica layer prepared from base-based precursor with pH $\approx$ 5 and annealed in H_2.

Magnetic properties of Fe-containing silica layers grown on Si substrates from the precursors used for bulk samples were quite close to those observed for bulk samples with respect to coercive force and the absence of saturation in the $M(H)$ dependence. The coercive force was equal to ≈ 400 and ≈ 700 Oe at 5 K and the blocking temperature was near 200 and 350 K for samples annealed in Ar and H_2, respectively. The $M(H)$ dependences were close to those for their bulk counterparts. The peculiarity observed at 50 K in the $M(T)$ dependence for H_2-annealed samples was similar to that [14] determined for nanostructures in mesoporous silica matrix. It should be remarked that $M(H)$ and $M(T)$ dependences were close to those for the layers prepared from precursors of a higher acidity (pH $\approx$ 2) [11].

3.3. Porous Fe-doped silica layers prepared with surfactant

Figure 5 shows the SEM micrographs of the samples prepared from TEOS solution with surfactant CTAB. On the surface of silica layer pores of 20–100 nm were observed, the number of which increased after annealing of the samples in air. Iron and iron oxides were most presumably located at pores and large defects of size ≈ 1 μm. Direct measurements of cross-sections indicated that the layers were not homogeneous with thickness varying in the range 30–80 nm.

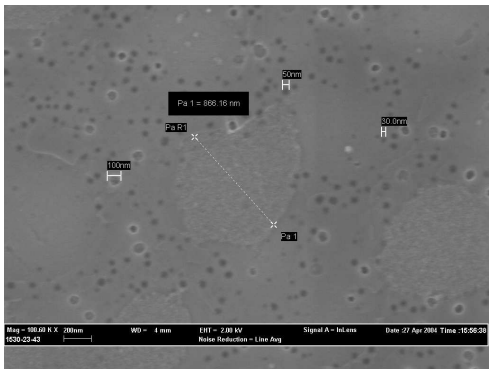

Fig. 5. SEM micrograph of Fe-containing silica layers prepared from TEOS solutions with surfactant CTAB after annealing. Bar denotes 100 nm.

Null-ellipsometry measurements have shown a large porosity in this series of samples. The estimated values of refractive indexes at 633 nm were equal to 1.32 and 1.39 for dried and annealed samples, respectively. A significant absorption should be mentioned which was indicated from the estimated values of imaginary part of dielectric function ε_2 equal to ≈ 0.2 for dried layers and ≈ 0.1 for annealed ones. Direct studies of coating solutions deposited on glass substrates have shown the absorption threshold at ≈ 2 eV with a strong peak at ≈ 3.4 eV. These optical features are typical of Fe_2O_3 [12]. A further absorption increase could be due to the presence of Fe_3O_4 [13].

Spectroscopic ellipsometry studies have shown that the spectra can be modeled by several layers of thickness 5–50 nm each presenting the contributions of Lorentzian-type lines. As followed from fitting procedure, the optical features were located at 1.0, 1.9, 3.3, and 4.6 eV. These energies were in agreement with characteristic features in Fe_2O_3 [12] and Fe_3O_4 [13]. The high-energy feature was stronger in annealed sample indicating an increased contribution of Fe_3O_4.

The magnetization of this type of Fe-doped silica layers appeared to be so small that it was impossible to estimate it even roughly on a strong background of substrate contribution. The small value or absence of Fe contribution could be caused by either low amount of iron/iron oxide in these very thin layers or by a singular Fe state in this case.

Summarizing, the structural, magnetic and optical studies have shown that the physical properties of Fe-containing silica layers can be efficiently changed by varying the porosity of medium. The size of formations containing iron and iron oxides was in the range from 20 nm to 50 μm and was strongly influenced by the porosity of silica layers.

Acknowledgments

This work was partly supported by EP6 project PHOREMOST N 511616.

References

[1] R.F. Ziolo, E.P. Giannelis, B.A. Weinstein, M.P. O'Horo, B.N. Ganguly, V. Mehrota, M.W. Russel, D.R. Huffman, *Science* **257**, 219 (1992).

[2] C. Caiser, C. Savii, M. Popovici, *Mater. Sci. Eng. B* **97**, 129 (2003).

[3] S. Lian, E. Wang, Z. Kang, Y. Bai, L. Gao, M. Jiang, C. Hu, L. Xu, *Solid State Commun.* **129**, 485 (2004).

[4] X. Wang, X. Chen, X. Ma, H. Zheng, M. Ji, Z. Zhang, *Chem. Phys. Lett.* **384**, 391 (2004).

[5] S. Solinas, G. Piccaluga, M.P. Morales, C.J. Serna, *Acta Mater.* **49**, 2805 (2001).

[6] F. del Monte, M.P. Morales, D. Levy, A. Fernandez, M. Ocana, A. Roig, E. Molins, K. O'Grady, C.J. Serna, *Langmuir* **13**, 3627 (1997).

[7] G.F. Goya, T.S. Berquo, F.C. Fonseca, M.P. Morales, *J. Appl. Phys.* **94**, 3520 (2003).

[8] D.L. Peng, T. Hihara, K. Surmiyama, H. Morikawa, *J. Appl. Phys.* **92**, 3075 (2002).

[9] M. Wu, Y.D. Zhang, S. Hui, T.D. Xiao, S. Ge, W.A. Hines, J.I. Budnick, M.J. Yacaman, *J. Appl. Phys.* **92**, 6809 (2002).

[10] M.F. Casula, A. Corrias, G. Paschina, *J. Non-Cryst. Solids* **293-295**, 25 (2001).

[11] I. Šimkiene, J. Sabataityte, J. Babonas, A. Reza, R. Szymczak, H. Szymczak, M. Baran, M. Kozlowski, S. Gierlotka, *Proc. SPIE*, accepted for publication.

[12] N. Ozer, F. Tepehan, *Solar Energy Mater. Sol. Cells* **56**, 141 (1999).

[13] W.F. Fontijn, P.J. van der Zaag, M.A.C. Devillers, V.A.M. Brabers, R. Metselaar, *Phys. Rev. B* **56**, 5432 (1997).

[14] K.S. Napolsky, A.A. Eliseev, A.V. Knotko, A.V. Lukashin, A.A. Vertegel, Yu.D. Tret'yakov, *Mater. Sci. Eng. C* **23**, 151 (2003).